Scaling of electric field fluctuations associated with the aurora during northward IMF

B. V. Kozelov[1] and I. V. Golovchanskaya[1]

Received 7 August 2006; accepted 20 September 2006; published 26 October 2006.

[1] We present a statistical study of scaling features of the electric field fluctuations measured by the DE2 satellite in the polar region during positive Bz IMF when the theta-aurora was observed by the DE1 satellite. It is demonstrated that the power spectra of the fluctuations have a power-law form at spatial scales from ~0.5 km (the limit of resolution) to several thousands of kilometers, with a break near 100 km. The scaling properties of the field are studied by examining the generalized structure functions (GSFs) and probability density functions (PDFs) of the fluctuations. The observed PDFs have a non-Gaussian shape with heavy tails. We also demonstrate a collapse of the re-scaled PDFs onto a single curve. A relation of PDF shape to solar wind conditions is revealed. The same analysis is performed on the TV observations of the theta-aurora. The scaling characteristics of the field and auroral fluctuations are compared. **Citation:** Kozelov, B. V., and I. V. Golovchanskaya (2006), Scaling of electric field fluctuations associated with the aurora during northward IMF, *Geophys. Res. Lett.*, *33*, L20109, doi:10.1029/2006GL027798.

1. Introduction

[2] Since the work of *Kintner* [1976], the turbulent properties of the high-latitude electric and magnetic fluctuations observed by the spacecraft in the ULF, ELF ranges have been repeatedly addressed. By now, after some controversy, it has been accepted that the observed frequencies of the fluctuations are Doppler shift frequencies in the satellite reference frame resulting from a satellite's motion through predominantly electrostatic coherent structures [*Tam et al.*, 2005, and references therein]. There is evidence of a cause-to-effect relationship between the turbulence displayed in the electric and magnetic fields and auroral structuring [*Frank et al.*, 1986; *Golovchanskaya et al.*, 2002]. As was convincingly demonstrated by *Frank et al.* [1986] for all cases when simultaneous optical observations were available, the most intense spikes in the fluctuating fields observed by DE2 were coincident with the occurrence of auroral arcs. A similarity between the turbulence and discrete auroral features with respect to the global distribution, seasonal variation, relation to solar wind, IMF and geomagnetic conditions has been pointed out by *Heppner* [1973], *Saflekos and Potemra* [1978], *Golovchanskaya et al.* [2002], and *Matsuo et al.* [2003]. Recently, *Tam et al.* [2005] have performed intermittency analysis on the electric field data obtained by a sounding rocket in the auroral zone. By examining the PDF and local intermittency measure, they evidenced the intermittent turbulence for the broadband ELF electric field fluctuations and showed that the degree of intermittency is larger at smaller scales. Only one event of intermittent fields was considered, without reference to solar wind and geophysical conditions.

[3] In the present study, by means of scaling analysis, we extend the investigation of the turbulence for the case when it develops in the polar region and is accompanied by polar cap theta aurora. Taking into account the arguments of *Borovsky* [1993] that auroral structuring can proceed on the scales as small as 100 m, we use the electric field measurements by the VEFI on DE2 at the top of resolution, that is 1/16 s. Under the assumption that the observed field variations are due to the spacecraft motion through quasi-stationary spatial structures (the DE2 velocity is ~7,5 km/s), this corresponds to the spatial resolution of ~500 m.

[4] Further, in section 2, we examine the GSFs and PDFs of the electric field fluctuations observed by DE2 in ten events of theta-aurora in the polar region during steadily northward Bz IMF. Such features as power-law relations for the GSFs, deviation of the PDFs from Gaussianity and collapse of the re-scaled PDFs onto a single curve are emphasized. In section 3, in order to demonstrate similarity between the scaling characteristics for the turbulent electric fields and optical auroras, we apply the scaling analysis to the TV observations of theta-aurora at Barentsburg (Svalbard). The principal results are summarized in section 4.

2. Scaling Properties of Electric Field Fluctuations

[5] We test for scaling properties the large-amplitude electric field fluctuations in the polar region registered by DE2 during prolonged intervals of positive Bz IMF and associated with theta-aurora, as evidenced by the UV imager of DE1. For October–November 1981, we found ten such intervals, which are summarized in Table 1. We assume that the state of the magnetosphere-ionosphere system is the same during each time interval selected and can be characterized by the magnitudes of Bz IMF and |B| IMF which we take from the OMNI database and average over each time interval (see Table 1). All DE2 crossings of the polar region that we consider were approximately in the dawn to dusk direction.

[6] One selected interval is from 10:00 to 19:00 UT on October, 17, 1981. During this period there were six passes of DE2 into the northern polar region. In order to enlarge the number of samples N (given in Table 1), we combined the observations at INV LAT from 60° to 84° in all six passes in one data domain (Figure 1, top plot). The electric power spectrum for this data set is shown in Figure 1,

[1]Polar Geophysical Institute, Apatity, Russia.

0094-8276/06/2006GL027798

Table 1. Results of Scaling Analysis of the Electric Field Fluctuations Observed by DE-2 Satellite

Date	N	$\langle\lvert B\rvert\rangle$, nT	$\langle Bz\rangle$, nT	S_1, km	α_1	α_2	α	w_1	w_2
12/10	140000	7	4	100	1.92 ± 0.04	1.30 ± 0.06	0.45	1.5	11.
16/10	178000	9	8	100	1.89 ± 0.02	1.57 ± 0.06	0.42	2.0	12.
17/10	125000	15	12	100	1.90 ± 0.01	1.50 ± 0.04	0.48	3.0	23.
25/10	52000	11	8	40	2.47 ± 0.01	1.29 ± 0.06	0.50	2.2	19.
31/10	250000	6	3	100	1.93 ± 0.02	1.32 ± 0.05	0.46	1.8	12.
08/11	92000	16	8	100	1.93 ± 0.05	1.29 ± 0.06	0.42	2.3	26.
12/11	72000	12	4	6, 100	2.00 ± 0.03	1.38 ± 0.04	0.38	2.0	15.
13/11	140000	10	3	8, 100	2.17 ± 0.03	1.33 ± 0.05	0.46	1.8	10.
25/11	160000	26	15	100	1.86 ± 0.02	1.35 ± 0.05	0.46	2.5	27.
26/11	210000	6	0	100	2.16 ± 0.03	1.73 ± 0.07	0.52	2.0	11.

bottom plot. The spectra are constructed by continuous wavelet transform of the data, with using the Morlet wavelet of the sixth order. The spectra exhibit a broken power-law form, with a break at $\lambda_1 \sim 100$ km. As seen from Table 1, the power-law indices α_1 at scales $< \lambda_1$ vary around the mean value $\langle\alpha_1\rangle = 2.0 \pm 0.2$; at larger scales they are smaller, $\langle\alpha_2\rangle = 1.4 \pm 0.2$. Here the errors of the mean values are given, while Table 1 contains the standard deviations of the values calculated from the least-square fits. Eight of the ten spectra do not have any break in the transition from MHD scales to kinetic scales (roughly a few km). In other two spectra there is a break at the point between MHD scales and kinetic scales.

[7] To test the electric field fluctuations δE for intermittency, we first study their scaling properties by constructing the GSF [*Frisch*, 1995], which for our problem is defined as $S_m(s) = \langle|\delta E(x, s)|^m\rangle$, where $\delta E(x, s) = E(x + s) - E(x)$, and the angle brackets imply averaging over x. To avoid the influence of extreme fluctuations, which results in statistically meaningless tails of the distribution, we use the conditioning technique [*Hnat et al.*, 2003]. Under conditioning, the GSF can be expressed via the PDF of fluctuations as

$$S_m(s) = \int_{-A}^{A} |\delta E|^m P(\delta E, s) d(\delta E)$$

Here the choice of the threshold A is based on the standard deviation of electric field fluctuations at a given scale s, $A(s) = K\,\sigma(s)$. In our consideration we adopted $K \geq 5$.

[8] If fluctuations δE exhibit scaling features with respect to the scale s, then $S_m(s) \propto s^{\zeta(m)}$. This appears to be the case for the electric field fluctuations being examined. From Figure 2 (inset), which shows S_m (m = 1, 2…6) for DE2 observations on October, 17, one can see a power-law form at scales up to a few tens of kilometers, so that we can estimate the scaling indices $\zeta(m)$. If it were $\zeta(m) = \alpha\, m$ with α being constant, then the fluctuations would statistically be self-similar with a single scaling exponent α. The plot of ζ as a function of m (Figure 2), however, indicates a deflection of the function $\zeta(m)$ from the linear relationship, signifying the presence of intermittency in the signal [*Frisch*, 1995]. At the same time, it is seen that the dependencies are closer to the linear relation for smaller A value, for which the conditioning technique preserves the less intermittent part of fluctuations.

[9] Now, we directly demonstrate for our dataset the deviation of the PDF $P(\delta E,s)$ from Gaussianity, as well as the collapse onto a single curve of the re-scaled PDFs $P_s(\delta E/s^\alpha) = s^\alpha P(\delta E, s)$ for different scales s. We find the scaling index α in two manners: from log-log plot of $P(0, s)$ versus scale s and from the first orders GSF (m = 1, 2, 3) as $\alpha = \zeta(\mathrm{m})/\mathrm{m}$. Both techniques yield nearly the same value of α. Further for definiteness we will use $\alpha = \zeta(2)/2$. The values of the scaling index α for the events considered are shown in Table 1. The index varies from 0.38 to 0.52, with the average value equal to 0.46 ± 0.04.

[10] An example of the re-scaled PDFs, exhibiting collapse in accordance with the relation $P_s(dX_s) = s^\alpha P(\delta E, s)$, where $dX_s = \delta E/s^\alpha$, is presented in Figure 3, top plot. One can clearly see non-Gaussianity of the collapsed PDF, as well as of individual PDFs constructed for different scales. It can be concluded that the large fluctuations are more probable than one would expect from the normal distributions, and this is a typical feature of the intermittent turbulence. However, the larger the scale, the narrower the region covered by the PDF on the collapsed curve. This is in agreement with the inverse variation of the intermittency measure with the scale previously reported by *Tam et al.* [2005].

[11] To characterize the shape of the collapsed PDF, we use its widths at the levels of 0.1 and 0.001, denoted as w_1

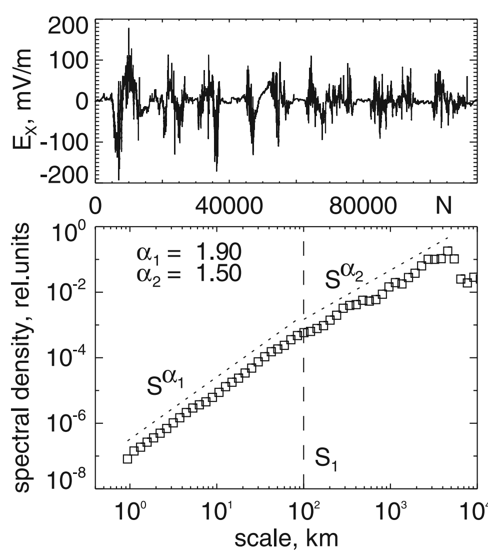

Figure 1. (top) Along-track electric field component E_x observed in DE2 crossings of the polar region during the event of October, 17, 1981. (bottom) Power spectrum of the E_x fluctuations over spatial scale.

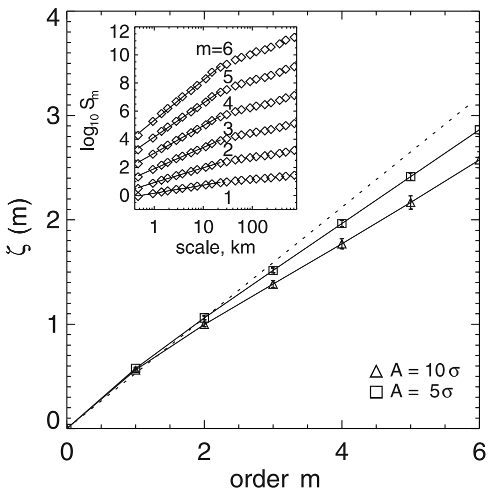

Figure 2. Scaling exponent of the conditioned GSF as a function of moment order for E_x fluctuations during the event of October, 17, 1981, the conditioning parameter A taken 10σ (squares) and 5σ (triangles). Uncertainty bars mark the standard deviations estimated for the slope of the power-law regions of the GSF S_m vs. scale. Inset shows the conditioned GSF vs. scale for $A = 5\sigma$.

and w_2 in Table 1. We have not found any appropriate functional fitting for the curve that could be meaningfully interpreted and thus use these empirical characteristics. We find out that the characteristic widths of the collapsed distributions are clearly dependent on the magnitude of the interplanetary magnetic field (Figure 3, bottom plot). Here, the uncertainty bars have been obtained from the deviation of points around the re-scaled PDF at the chosen levels. There is a dependence on the Bz IMF as well, but it is not so well pronounced. The relation of the electric field turbulence to the Bz IMF was earlier revealed by *Golovchanskaya et al.* [2002]. The IMF dependence of PDF

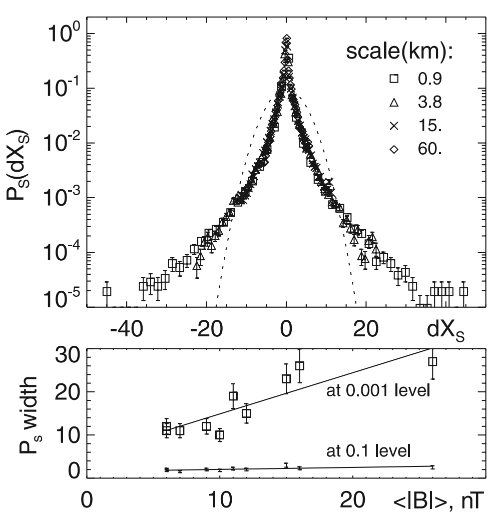

Figure 3. (top) Re-scaled PDFs of E_x fluctuations at different scales during the event of October, 17, 1981; dotted line is a Gaussian PDF. (bottom) The width of the collapsed PDF of E_x fluctuations depending on the average |B| IMF.

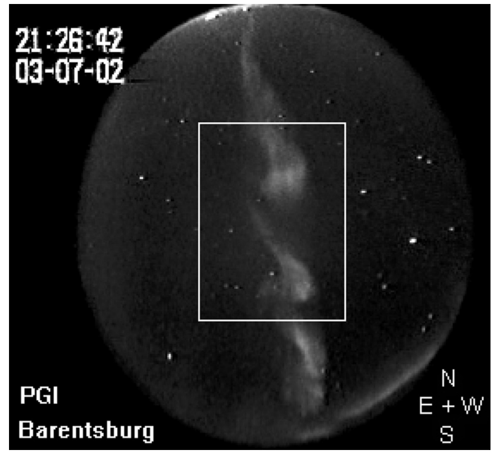

Figure 4. Spatial structure of the transpolar arc.

shape can be explained if we assume that the turbulence under study is associated with the Birkeland field-aligned currents/large-scale convection velocity shears. Since these currents are strongly controlled by the IMF, the properties of the turbulence can also be IMF dependent.

3. Scaling Analysis Applied to the TV Observations

[12] Barentsburg observatory is located at Svalbard, the quiet nighttime auroral oval being observed near its southern horizon. This location is very favorable for observations of transpolar arcs. These arcs are believed to be related to the plasma sheet and appear most commonly during northward IMF conditions. Unfortunately, no TV observations were performed during DE2 mission. However, as the theta-aurora is a regular phenomenon associated with positive Bz IMF, we simply take an event from our database. We choose for the analysis an activation of the transpolar arc observed on March, 7, 2002 from 21:15 to 21:30 UT. Some details of this event were previously described by *Kornilov et al.* [2005].

[13] The digitized video frames (25 frames per second) from television all-sky camera (TV ASC) are superposed and averaged over 1 s to reduce the noise level. The central part of the frames, $\sim$200 $\times$ 200 km^2, where projection distortions are not significant, is analyzed (Figure 4). The spatial resolution of the TV ASC in the center of the field of view for the altitude of the aurora ($\sim$110 km) is $\sim$1.2 km and changes for $\sim$1.7 km toward the boundary of the central part of the frame that we treat. We consider a two-pixel variation $dI = I(p + ds) - I(p)$ of the intensity I, for a given vertical and horizontal distance ds in each frame. The data from 100 successive frames are combined to improve the statistics. Thus we have more than 10^6 points to construct the distributions.

[14] The average spatial resolution of the TVASC in the considered field of view is $\sim$1.5 km (here the variations in the spatial resolution and other distortions of ASC image are ignored), so we can directly obtain the spatial structure function at a given time.

[15] An example is illustrated in Figure 5, top plot. From the inset plot in Figure 5 (top) one can see that the conditioned structure functions of the considered moments

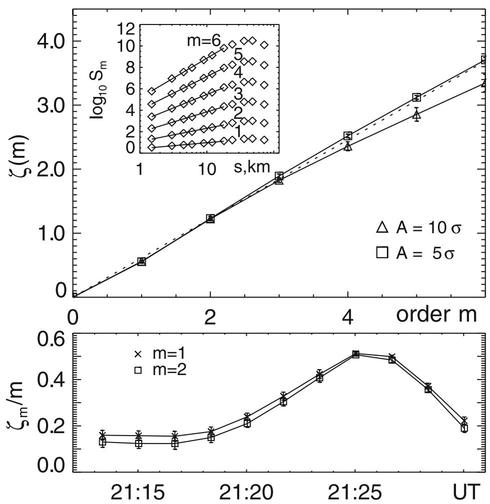

Figure 5. (top) Same as in Figure 2 but for the spatial fluctuations of auroral intensity at 21:25:52–21:27:32 UT. (bottom) Evolution of the scaling exponents of the GSF for the first two orders in the course of the transpolar arc development.

have a well-defined power-law form in the range from 1.5 km to 25 km. The power-law indices $\zeta(m)$, which are plotted as a function of the moment, indicate nearly a linear relationship for the first three moments but for the higher moments the linearity of $\zeta(m)$ does not hold. The application of the conditioning technique [*Hnat et al.*, 2003] with the thresholds $A \geq 8\sigma$ (not shown) does not change the character of the dependence. Only with the threshold less than $A = 5\sigma$, the dependence approaches the linear relation. On this ground, we conclude that the signal under study has a multifractal intermittent structure.

[16] It is interesting to note that in the course of the event it is possible to follow the temporal evolution of the scaling indices (Figure 5, bottom plot). It appears that the normalized index ζ_m/m for m = 1,2 gradually varies from ~0.15 for the weak homogeneous arc at the early stage to 0.53 for the disturbed arc at the late stage of evolution. The disturbance is displayed as a southward motion of the vortex-like structures along the arc (see Figure 4). Thus we can assume that the temporal evolution of the scaling indices is a manifestation of the development of some instability which may be included in the scenario proposed by *Chang et al.* [2004].

[17] The analysis of the PDF for the fluctuations of the auroral intensity is more complicated than for electric field fluctuations because of interference of noise in the TV system, starlight and airglow. However these sources yield Gaussian PDFs, which is evidenced by the PDFs obtained in the absence of aurora. When aurora appears in the TV ASC field of view, we can see a deviation of the PDF of auroral intensity fluctuations from this simple form to a more stretched one. A more detailed examination of the PDF is a subject of further studies, here we only point out that at each moment of arc activation it is possible to collapse the PDFs for scales from 1.5 km to ~20 km onto a single curve. A typical example of the collapse is given in Figure 6.

[18] A similarity of the characteristics of the GSFs and PDFs constructed for structured electric fields and for optical auroras gives more evidence for close association of these two manifestations.

4. Summary

[19] By implying a close relationship between the high-latitude electric turbulence and auroral arcs, we easily found the events of strong turbulent electric fields in the polar region during steadily northward Bz IMF, when theta-aurora and transpolar arcs were observed. To examine these fields, we applied the technique of the generalized structure function and probability density function, and demonstrated that they generally have scaling properties similar to those of the turbulent electric fields in the auroral zone [*Tam et al.*, 2005]. The observed scaling features are in a good agreement with the scenario proposed by *Chang et al.* [2004]. It induces intermittent turbulence by a dynamical topological complexity that results from the nonlinear evolution of magnetic and plasma coherent structures arising from plasma resonances and consisting of bundles of non-propagating fluctuations. In order to give more evidence for the association between the turbulent fields and auroras, we applied the same technique to optical observations of theta-aurora and found a close similarity in the scaling characteristics of optical and electric field data.

[20] For the electric field fluctuations, we have shown that the scaling index α is not constant and varies over a wide range 0.38 $\div$ 0.52. That is different from the predictions of Kolmogorov's theory (α = 1/3) and Kraichnan's theory (α = 1/4 [*Kraichnan*, 1967]). However, the theories describe a stationary situation. From applying the scaling analysis to auroral data we have seen that the scaling index α is changing during the event. This fact remains to be understood and addressed by the theory.

[21] Finally, we note that all results of the present study have been obtained without discriminating between the fluctuations on the closed magnetic field lines (CFLs) and open field lines (OFLs). Actually, the preliminary analysis of those DE2 passes where we were able to discriminate between the CFLs and OFLs more or less unambiguously

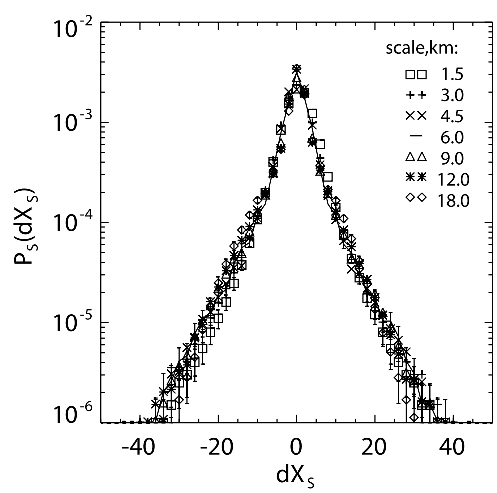

Figure 6. Re-scaled PDFs of auroral intensity fluctuations at 21:25:52–21:27:32 UT for various scales.

by invoking DE2 particle data, indicated that the main spectral and scaling features of the turbulent electric fields on the CFLs and OFLs are qualitatively the same. That is, the broken power-law spectra, leptokurtic shape of the PDFs and collapse of the re-scaled PDFs keep in both cases. In the future, this point should be addressed more in detail.

[22] **Acknowledgments.** Authors acknowledge the NASA National Space Science Data Center and Dr. Nelson C. Maynard for VEFI data used. The work was partly supported by the Presidium of the Russian Academy of Sciences (RAS) through the basic research program "Solar activity and physical processes in the Sun-Earth system" and by the Division of Physical Sciences of RAS through the program "Plasma processes in the solar system."

References

Borovsky, J. E. (1993), Auroral arc thicknesses as predicted by various theories, *J. Geophys. Res.*, *98*, 6101–6138.

Chang, T., S. W. Y. Tam, and C. C. Wu (2004), Complexity induced anisotropic bimodal intermittent turbulence in space plasmas, *Phys. Plasmas*, *11*, 1287–1299.

Frank, L. A., et al. (1986), The theta aurora, *J. Geophys. Res.*, *91*, 3177–3224.

Frisch, U. (1995), *Turbulence: The Legacy of A. N. Kolmogorov*, 89 pp., Cambridge Univ. Press, New York.

Golovchanskaya, I. V., Y. P. Maltsev, and A. A. Ostapenko (2002), High-latitude irregularities of the magnetospheric electric field and their relation to solar wind and geomagnetic conditions, *J. Geophys. Res.*, *107*(A1), 1001, doi:10.1029/2001JA900097.

Heppner, J. P. (1973), High-latitude electric fields and the modulations related to interplanetary magnetic field parameters, *Radio Sci.*, *8*, 933–948.

Hnat, B., S. C. Chapman, G. Rowlands, N. W. Watkins, and M. P. Freeman (2003), Scaling in long term data sets of geomagnetic indices and solar wind ε as seen by WIND spacecraft, *Geophys. Res. Lett.*, *30*(22), 2174, doi:10.1029/2003GL018209.

Kintner, P. M., Jr. (1976), Observations of velocity shear driven plasma turbulence, *J. Geophys. Res.*, *81*, 5114–5122.

Kornilov, I. A., T. A. Kornilova, and O. I. Kornilov (2005), Some aspects of polar arc generation process, paper presented at XXVIII Annual Seminar "Physics of Auroral Phenomena," Polar Geophys. Inst., Apatity, Russia. (Available at http://pgi.kolasc.net.ru/seminar/archive/2005/Proceedings/1_storm/Kornilov_4.pdf)

Kraichnan, R. H. (1967), Inertial ranges in two-dimensional turbulence, *Phys. Fluids*, *10*, 1417–1423.

Matsuo, T., A. D. Richmond, and K. Hensel (2003), High-latitude ionospheric electric field variability and electric potential derived from DE-2 plasma drift measurements: Dependence on IMF and dipole tilt, *J. Geophys. Res.*, *108*(A1), 1005, doi:10.1029/2002JA009429.

Saflekos, N. A., and T. A. Potemra (1978), Small-scale transverse magnetic disturbances in the polar regions observed by TRIAD, *J. Geophys. Res.*, *83*, 1493–1502.

Tam, S. W. Y., T. Chang, P. M. Kintner, and E. Klatt (2005), Intermittency analyses on the SIERRA measurements of the electric field fluctuations in the auroral zone, *Geophys. Res. Lett.*, *32*, L05109, doi:10.1029/2004GL021445.

I. V. Golovchanskaya and B. V. Kozelov, Polar Geophysical Institute, Apatity, Murmansk, 184209 Russia. (kozelov@pgi.kolasc.net.ru)